

ORIGINAL RESEARCH

Phase coded waveforms for integrated sensing and communication systems

Sevda Şahin | Tolga Girici 

Electrical and Electronics Engineering, TOBB
University of Economics and Technology, Ankara,
Türkiye

Correspondence

Tolga Girici, Electrical and Electronics Engineering,
TOBB University of Economics and Technology,
Çankaya, Ankara, 06510, Türkiye.
Email: tgirici@etu.edu.tr

Abstract

Nowadays, especially with the developments in the automotive industry, it has become a highly popular topic for radar and communication systems to operate on the same platform and perform joint tasks to increase situational awareness. Sharing the hardware of the radar and communication systems and using a joint waveform for both functions eliminate interference problems between the systems, increasing the effectiveness of the joint task. In studies where radar signals are utilised for communication functions, continuous wave frequency modulation or intra-pulse frequency modulation is generally employed to transmit communication signals. There are a few studies in the literature on joint radar and communication waveforms using phase modulation. In these studies, phase modulation is not employed directly for both functions. As a contribution to the literature, this study evaluates the usage of joint radar and communications waveforms, such as Barker sequences and Zadoff–Chu sequences as opposed to linear frequency modulation. We compare these waveforms terms of range-speed detection and symbol error rate.

KEYWORDS

automotive radar, data communication, radar, radar detection, radar waveforms

1 | INTRODUCTION

As autonomous systems become widespread in both military and civilian areas, the importance of situational awareness for these systems is increasing. To enhance situational awareness, radars are being used more frequently in military applications, including air defence systems, command control systems, and early warning systems as well as in civilian applications such as air traffic control, remote sensing, automobile speed control and collision avoidance systems. On the other hand, the rising data rate requirements in wireless communication systems have led to an increase in the bandwidth of communication systems. Consequently, this has caused the operating frequencies to approach those of radar systems. This situation has led to electromagnetic interference between the communication and radar systems on the same platform [1]. Methods such as spectrum sharing and common waveform use are suggested in various studies to overcome this problem [2–4]. In this study, we focused on the utilisation of joint waveforms. The

definition of joint waveforms typically involves the use of existing radar or communication waveforms. In both scenarios, the transmitted waveform undergoes random changes depending on the communication signal it carries. While this random characteristic is expected in communication systems, it poses challenges for radar systems. Radar systems operate under the assumption that the signal reflected from the target area remains constant during the pulse integration period. The randomness in the transmitted waveform adversely affect the performance of the radar system. To enhance the radar target detection performance, which deteriorates due to the random characteristics of the communication symbols, the phase correction method is proposed in Alabd et al. [5]. We examined this method in detail in Şahin and Girici [6] and we proposed the matched filter bank method in order to minimise the effect of randomness of communication symbols on radar detection performance. In the method proposed in Şahin and Girici [6], aligned with the mono-static pulse radar operational concept, each received pulse at the radar receiver undergoes processing

This is an open access article under the terms of the [Creative Commons Attribution](https://creativecommons.org/licenses/by/4.0/) License, which permits use, distribution and reproduction in any medium, provided the original work is properly cited.

© 2024 The Author(s). *IET Radar, Sonar & Navigation* published by John Wiley & Sons Ltd on behalf of The Institution of Engineering and Technology.

by passing through a matched filter selected from the filter bank. These matched filters are compatible with the communication symbol sent by the transmitter. In the study referenced as Alabd et al. [5], communication symbols are transmitted using the Linear Frequency Modulated (LFM) radar waveform. As the LFM waveform involves a single phase transition during the transmission period of a communication symbol, the phase correction method proposed in Alabd et al. [5] can be applied, resulting in observed improvements in radar performance. However, this method is not suitable for phase-modulated waveforms with multiple phase transitions within the pulse, such as Barker coded and Zadoff–Chu coded pulses, making its application impossible. The utilisation of intra-pulse phase modulation waveforms as Integrated Sensing and Communications (ISAC) waveforms has been limited in the literature due to the negative effects on radar performance resulting from the randomness of communication symbols. In the study presented in Rafique and Arslan [7], Barker code has been utilised for the radar function, but the waveform with Barker code does not incorporate the modulation of communication symbols. On the other hand, in Gehre et al. [4], the Zadoff–Chu sequence is suggested for the ISAC system, yet the radar function waveform is not implemented with the portion containing Zadoff–Chu. In the study conducted in Rodriguez-Garcia et al. [3], the Barker coded waveform is used as the ISAC waveform, but the study describes a method to prevent unwanted receivers from detecting the communication signal in the operational scenario.

Our recent study, presented in Şahin and Girici [6], introduces the matched filter bank method, which can be applied to waveforms with intra-pulse phase modulation. In this current study, we applied the method proposed in Şahin and Girici [6] to assess the performances of both radar and communication systems for waveforms utilising intra-pulse phase modulation, providing a comprehensive analysis. We performed the analyses for pulse modulated radar. A mono-static radar is assumed in the joint communication and target sensing system.

In this study, new ISAC waveforms are proposed using Barker and Zadoff–Chu codes, contributing to the literature. Unlike previous studies, radar and communication functions utilising the entire waveform have been defined, as opposed to utilising separate regions for radar and communication functions. Consequently, the entire bandwidth of the waveform could be utilised for both radar and communication functions. Radar target range and velocity estimation performance analyses and comparisons of both waveforms were made and compared with ISAC waveform that uses frequency modulation on pulse for a mono-static pulse radar operational concept (Figure 1). In addition, the symbol error rate (SER) in the communication receiver was also examined.

2 | ISAC SYSTEM WAVEFORM DESIGN

Within the scope of this study, a new waveform was proposed as the intra-pulse phase modulated ISAC waveform, primarily using the Barker code. The performance of this waveform was

compared with the LFM ISAC waveform proposed in ref. [2]. Subsequently, another phase-modulated ISAC waveform was generated using the Zadoff–Chu sequence and its performance were compared with that of the Barker-coded ISAC waveform. Performance analyses were conducted for both the radar and communication systems.

2.1 | ISAC waveform—Linear Frequency Modulated

An LFM radar signal with pulse width τ , bandwidth B and initial phase ϕ_0 is expressed by (1) [5].

$$S_{chirp}(t) = e^{j(\pi\mu t^2 + 2\pi f_0 t + \phi_0)} \quad (1)$$

Here f_0 is the carrier frequency and $\mu = \frac{B}{\tau}$ is the chirp rate. Also, t is an element of the set $[-\tau/2, \tau/2]$. In order to send the communication symbols within the radar pulse, different initial frequencies are used for the chirp signal for each symbol. As seen in Figure 2 in the ISAC system waveform, each pulse is divided into two and a chirp with a different initial frequency is used for each segment. The mathematical expression of this signal is given in (2).

$$S_{ISAC-LFM}(t) = S_{chirp}(t - \Delta t_m) \quad (2)$$

Δt_m is determined by $\Delta t_m = \frac{m\tau}{M}$, $m \in \{1, 2, \dots, M - 1\}$ Here, M is the number of symbols, where the number of bits/symbol is $\log_2 M$.

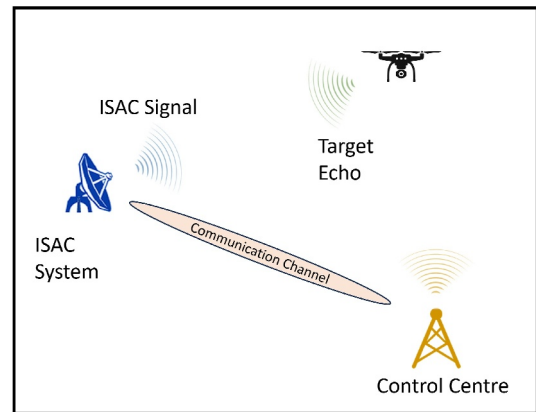


FIGURE 1 Operational concept illustration of joint communication and target sensing system.

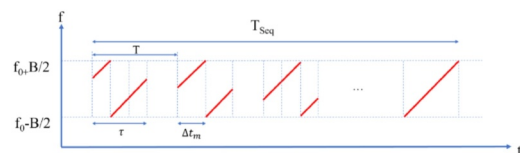


FIGURE 2 Chirp pulsed signal for the ISAC-LFM system. ISAC-LFM, Integrated Sensing and Communications-Linear Frequency Modulation.

2.2 | ISAC waveform—Barker

In radars with low detection probability, intra-pulse Barker code is used as a pulse compression technique [8,9]. Target detection is carried out after creating a cross-correlation between the received signal and the sent signal in a radar receiver. Since the peak to the side lobe ratio (PSL) in the autocorrelation function of Barker codes is low, target detection can be achieved with high accuracy in the radar using this code [10].

In the Barker code, the pulse width τ is divided into N sub-pulses, each with a width of $\tau_0 = \tau/N$. The phase of each sub-pulse is chosen as 0 or π . A sub-pulse with a phase of 0 is denoted as 1 or “+”, while a sub-pulse with a phase of π is denoted as 0 or “-”. The Barker code with a code length of 7 is illustrated in Figure 3 [11]. The Barker code of length N is expressed as BN .

The minimum PSL that can be achieved with the Barker code with a code length of 13 can be 22.3 dB (Table 1). However, in practice, the ratio required for radar signal processing is at least 30 dB [12]. To satisfy this requirement, the nested Barker code is used. The nested Barker code is generated by taking the Kronecker product of two Barker codes, and the length of the nested Barker code is the product of the lengths of the used Barker codes [10]. For example, the length of the nested Barker code created using B7 and B4 Barker codes is 28. As a contribution, within the scope of this study, the nested Barker code was used to send communication symbols within the radar pulse. By using the nested Barker code, the minimum peak side beam level requirement at the radar receiver is satisfied and communication symbols can be sent within the radar pulses. In this context, in addition to the Barker codes given in Table 1 in the literature, it was

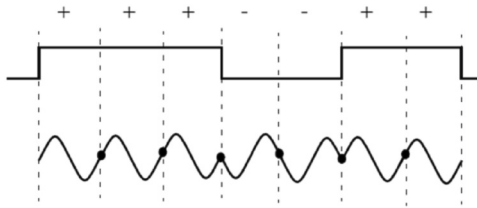


FIGURE 3 The Barker code with a code length of 7 (B_7).

TABLE 1 The Barker code with a code length of 7 (B_7).

Code	Length	Code elements	PSL (dB)
B_2	2	+-, ++	6.0
B_3	3	+++	9.5
B_4	4	+++-, +++-	12.0
B_5	5	+++++	14.0
B_7	7	+++--	16.9
B_{11}	11	+++--+-	20.8
B_{13}	13	++++-+-	22.3

Abbreviation: PSL, peak to the side lobe ratio.

investigated whether there were other codes with the same code length. It has been determined that the Barker code with code length 4 has [+ - + +] and [- + + +] Barker code features in addition to the code elements given in Table 1 (3).

$$\begin{bmatrix} B_{4_1} \\ B_{4_2} \\ B_{4_3} \\ B_{4_4} \end{bmatrix} = \begin{bmatrix} + & + & + & - \\ + & + & - & + \\ + & - & + & + \\ - & + & + & + \end{bmatrix} \quad (3)$$

Using the four B4 codes given in (3) and the B11 code provided in Table 1, four B44 codes can be generated for a two-bit communication data (4).

$$\begin{bmatrix} m_1 \\ m_2 \\ m_3 \\ m_4 \end{bmatrix} = \begin{bmatrix} B_{4_1} \otimes B_{11} \\ B_{4_2} \otimes B_{11} \\ B_{4_3} \otimes B_{11} \\ B_{4_4} \otimes B_{11} \end{bmatrix} \quad (4)$$

When the Kronecker product is taken with a specific code sequence from the code sequence given in Equation (2) for each communication symbol, the intra-pulse chip count, that is, the instantaneous bandwidth of the joint waveform, can be increased as given in (5).

$$\begin{bmatrix} m_1 \\ m_2 \\ m_3 \\ m_4 \end{bmatrix} = \begin{bmatrix} (B_{4_1} \otimes B_{11}) \otimes B_5 \\ (B_{4_2} \otimes B_{11}) \otimes B_5 \\ (B_{4_3} \otimes B_{11}) \otimes B_5 \\ (B_{4_4} \otimes B_{11}) \otimes B_5 \end{bmatrix} \quad (5)$$

The joint waveform for the ISAC system was generated as given in (5).

2.3 | ISAC waveform—Zadoff–Chu

Zadoff–Chu (ZC) arrays are a fundamental waveform used to generate the spread spectrum in modern cellular systems, including long-term evolution (LTE) and 5G new radio. They largely replace the foundational Pseudo-Noise (PN) and Walsh sequences of the 3G cellular era and the 2G IS-95. Unlike real and binary-valued Walsh and PN codes commonly used in communication systems, ZC sequences are complex sequences with unit magnitude and specific phase shifts, most commonly ± 1 [13].

A ZC array has two basic parameters: root index $q = 1, 2, \dots, N_{zc} - 1$ and the length of the string, N_{zc} , which must be an odd number (and is often a prime number). Considering these two parameters, the q^{th} ZC sequence $s_q[n]$ is created as given in (6).

$$s_q[n] = e^{-j\pi q \frac{n(n+1)}{N_{zc}}} \quad (6)$$

Here, n is given as $0, 1, 2, \dots, N_{zc} - 1$. Zadoff–Chu sequences generated in this way are of constant amplitude, zero cyclic autocorrelation, fixed cyclic cross-correlation. Moreover,

Discrete Time Fourier Transform (DTFT) or Inverse Discrete Time Fourier Transform of a ZC Sequence is also a ZC Sequence [13].

When the advantages of these properties for the range and velocity estimation performance of the radar are considered, at this stage of the study, a joint waveform has been created for the ISAC system using (6). As a contribution, within the scope of this study, by using a different q value for different communication symbols, it is possible to send one communication symbol in each pulse.

3 | RECEIVER PROCESSING

3.1 | Communication receiver

The signal received by the communication receiver is given by (7). Here $w_k(t)$ represents additive white Gaussian noise.

$$y_k(t) = S_{RadCom}(t) + w_k(t) \quad (7)$$

The demodulation of this signal at the receiver is usually carried out using matched filtering. In this method, the cross-correlation of the received signal with all possible signature signals is calculated as $z_i(t) = \text{corr}(y_k(t), S_i(t))$, $i = 1, \dots, M$. Here, M is the number of symbols and $S_i(t)$ is the signature signal of the i^{th} symbol. In cross-correlation, the signature signal that gives the result with the highest peak value is accepted as the sent symbol [2]. Estimation of the sent symbol, i_{est} , is determined by $i_{est} = \text{argmax}_{i=1, \dots, M} (\max_f \{|z_i(t)|\})$.

3.2 | Matched filter bank ISAC radar receiver

In the matched filter bank technique, the radar pulses received at the receiver are passed through a matched filter which is compatible with the communication signal sent by the transmitter [6]. To achieve this, matched filters are used in the radar receiver as many as the number of symbols that can be sent from the transmitter, that is, M (Figure 4). When evaluating the impact of the number of matched filters on the radar receiver, we can consider parameters such as power consumption, time delay, weight, and size. Since only the relevant matched filter is used in processing the signal returned from the target on the radar receiver, the number of matched filters has no effect on power consumption or time delay in signal processing. It is sufficient to consider the power consumption and time delay of the switch used for selecting the matched filter, compared to a conventional radar receiver. However, the number of matched filters will increase the weight and size of the radar receiver. The importance of weight and size depends on the platform limitations of the ISAC system. For example, in an ISAC system on a platform with limited resources, such as a drone, the increase in weight and size due to the number of matched filters is a critical issue that needs

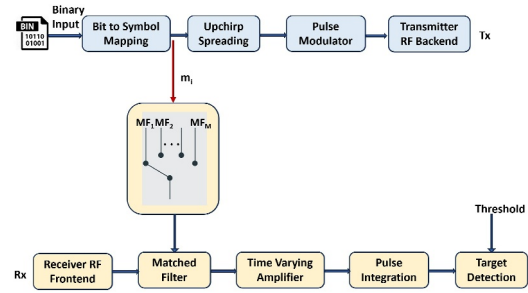


FIGURE 4 Block diagram for the matched filter bank ISAC radar. ISAC, Integrated Sensing and Communications.

careful consideration. However, in a ground-based air defence system, this increase may be negligible. In the implementation of the matched filter, an Acorn Reduced Instruction Set Computer Machine (ARM) processor, a microcontroller, Digital Signal Processing (DSP), or Field Programmable Gate Array (FPGA) can be used depending on the application platform and purposes of the ISAC system [14–17]. In the implementation of matched filters in a radar receiver, the choice between ARM processors, microcontrollers, DSPs, or FPGAs depends on the specific requirements of the ISAC system. ARM processors, with their ability to run an operating system, are ideal for multitasking environments where robust transaction management and control tasks are needed. Microcontrollers offer cheaper solution. DSPs excel in high-speed data processing tasks such as modulation, demodulation, encryption, and decryption, making them suitable for complex signal processing operations. FPGAs, on the other hand, offer flexibility in design and real-time processing capabilities, making them ideal for applications requiring parallel processing and frequent algorithm updates. While DSPs rely on software for signal processing, FPGAs implement these functions through hardware, allowing for faster data processing and adaptability in field conditions. The choice of technology—whether ARM, DSP, or FPGA—should be aligned with the specific control, processing speed, and flexibility needs of the radar system.

Matched filters for the ISAC-LFM system can be designed by using (8) for each communication symbols [6].

$$MF_i(t) = e^{2j\pi \left(\frac{0.5B}{\tau}\right) \left(\frac{t(i)}{f_s}\right)^2} \quad (8)$$

Here, f_s is the sampling rate and $t(i)$ can be calculated by using $t(i) = \text{mod}[K - k(i) - 1 + \mathbf{t}_i, K]$, where \mathbf{t}_i is the time index array, $K = \tau f_s$ and $k(i) = Km(i)/M$.

Matched filters for the ISAC-Barker system can be designed (9) for each communication symbols.

$$MF_i[n] = m_i^* e^{2j\pi f_0 n} \quad (9)$$

Here, $m_i^* = [B_N B_{N-1} \dots B_1]$ for a i^{th} communication symbol's Barker sequence $m_i = [B_1 B_2 \dots B_N]$ and f_0 is the carrier frequency of the transmitted signal.

Matched filters for ISAC–Zadoff–Chu system can be designed (10) for each communication symbols.

$$MF_i[n] = -\text{conj}\left(e^{-j\pi q_i \frac{n(n+1)}{N_{zc}}}\right) \quad (10)$$

Here, q_i is the root index of the i^{th} symbol.

4 | SIMULATIONS

By utilising the ISAC waveform recommended in Section 2, simulations were conducted in MATLAB following the monostatic operational scenario. The performances of both the radar and communication systems were first assessed for each ISAC waveform, and subsequently, they were compared for $M = 4$. The parameters used in the simulations are listed in Table 2. As given in Table 2, the ISAC–Barker waveform has a length of $20\mu\text{sec}$ and a chip duration of $\frac{20\mu\text{s}}{220} = 0.091\mu\text{ sec}$, which implies a bandwidth of 11 MHz, and similarly, the ISAC–Zadoff–Chu waveform has a length of $19.9\mu\text{sec}$ and a chip duration of $\frac{19.9\mu\text{s}}{219} = 0.091\mu\text{ sec}$, which implies bandwidths of 11 MHz. These are the same bandwidths as the ISAC–LFM signal, which means a fair comparison between ISAC waveforms.

After conducting these analyses, we incorporated Hamming windowing into the radar receiver to enhance the performance of phase-modulated ISAC waveforms and compared

the performance of all three ISAC waveforms. Subsequently, we introduced volume clutter into the scenario to assess the performance of phase-modulated ISAC waveforms in the presence of volume clutter and we analysed performances of ISAC waveforms without and with Hamming windowing.

4.1 | Radar performance analysis for waveforms

The simulations were conducted using ISAC waveforms proposed in Section 2.1, Section 2.2 for B220 and Section 2.3 for $N_{zc} = 219$. The estimation performance of the radar was examined when communication symbols were transmitted with radar pulses. Simulations were carried out using the matched filter bank method given in Section 3.2. The targets in the scenario are positioned at various ranges between 3 and 74 km. The speeds of the targets vary between -15 m/s and $+15\text{ m/s}$. The mean square error (MSE) of the range estimations and the MSE of the velocity estimations for each ISAC waveform are provided in Figures 5 and 6, respectively. As seen in Figure 5, based on the scenario parameters provided in Table 2, the range estimation error with ISAC–Barker and ISAC–Zadoff–Chu waveforms is higher than with ISAC–LFM for target ranges less than 10 km. Notably, ISAC–Zadoff–Chu exhibits superior performance compared to ISAC–Barker. On the other hand, as depicted in Figure 6, the velocity estimation performance of ISAC–Barker and ISAC–Zadoff–Chu is nearly identical, with both slightly better than ISAC–LFM. When intra-pulse phase-modulated waveforms are used, the Doppler shift caused by high-speed targets can lead to a phase shift in the signal reflected from the target, resulting in errors in target range estimation. However, in this scenario, the target speeds ranging from -15 m/s to $+15\text{ m/s}$ do not cause a significant decrease in range estimation performance of intra-pulse phase-modulated waveforms compared to LFM-modulated waveforms.

At this stage of the study, our focus was on improving the performance of ISAC–Barker and ISAC–Zadoff–Chu

TABLE 2 Simulation parameters.

Simulation parameters	Value
Radar carrier frequency, f_0	10GHz
Radar range	75km
Radar blind range for ISAC–LFM	3km
Radar blind range for ISAC–Barker	3km
Radar blind range for ISAC–Zadoff–Chu	2.98 km
Radar false alarm probability	10^{-6}
Modulation order, M	4
Radar pulse width for ISAC–LFM (τ)	$20\mu\text{s}$
Radar pulse width for ISAC–Barker (τ)	$20\mu\text{s}$
Radar pulse width for ISAC–Zadoff–Chu (τ)	$19.9\mu\text{s}$
Radar pulse repetition interval (T)	$500\mu\text{s}$
Data rate $\left(\frac{\log_2 M}{T}\right)$	4 kbps
ISAC–LFM bandwidth	11 MHz
Barker code length	$4 \times 11b \times 5$
ISAC–Barker bandwidth	11 MHz
Zadoff–Chu code length	219
ISAC–Zadoff–Chu bandwidth	11 MHz
Rain rate	2 mm/hr

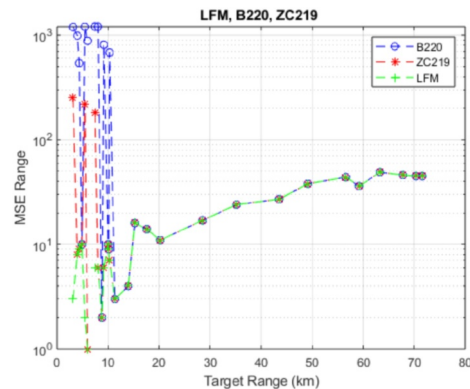


FIGURE 5 MSE range for ISAC–LFM, ISAC–Barker and ISAC–ZC, $M = 4$, $BW = 11\text{MHz}$, $f_0 = 10\text{GHz}$. ISAC, Integrated Sensing and Communications; ISAC–LFM, Integrated Sensing and Communications–Linear Frequency Modulation; ISAC–ZC, Integrated Sensing and Communications–Zadoff–Chu; MSE, Mean square error.

waveforms at low target ranges. When utilising these waveforms, side lobes were observed in the radar receiver's matched filter output due to the nature of Barker and Zadoff–Chu codes. As reflections from targets at close ranges result in high-amplitude signals reaching the receiver, the amplitude of these side lobes exceeded the threshold level, leading to incorrect range estimation. The received signal and the threshold level are shown in Figures 7 and 8 for short and long target ranges, respectively. To mitigate this effect, we applied a Hamming window to the signal reflected from the target at the radar receiver before processing. As can be seen in Figure 9, the performance of ISAC–Barker and ISAC–Zadoff–Chu waveforms at low target ranges has been improved by using the Hamming window. On the other hand, Figure 10 illustrates that the Hamming window has limited impact on the speed estimation performance of these waveforms.

At this stage of the study, we introduced an atmospheric environment with a rain rate of 2 mm/hr (moderate rain) to analyse the performance of ISAC–Barker and ISAC–Zadoff–Chu waveforms under the clutter effect, as specified in Table 2. As depicted in Figure 11, clutter negatively affects the

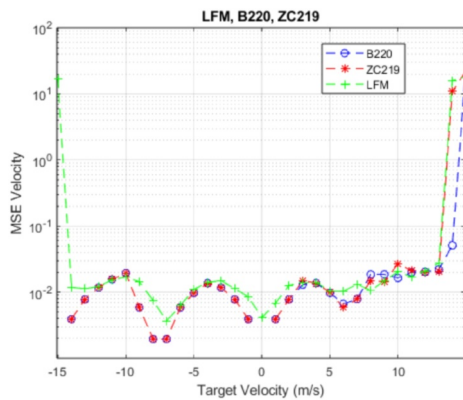


FIGURE 6 MSE velocity for ISAC–LFM, ISAC–Barker and ISAC–ZC, $M = 4$, $BW = 11\text{MHz}$, $f_0 = 10\text{GHz}$. ISAC, Integrated Sensing and Communications; ISAC–LFM, Integrated Sensing and Communications–Linear Frequency Modulation; ISAC–ZC, Integrated Sensing and Communications–Zadoff–Chu; MSE, Mean square error.

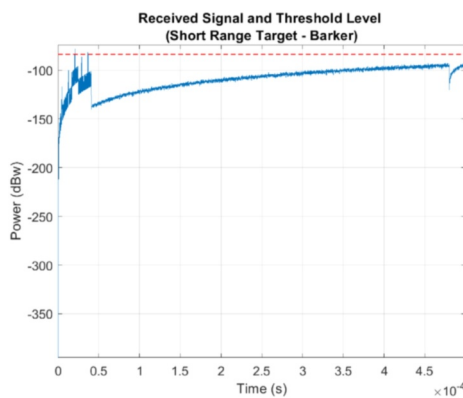


FIGURE 7 Received signal and threshold level for short range target—ISAC–Barker. ISAC, Integrated Sensing and Communications.

range estimation performance of all waveforms at low ranges. The degradation in performance under clutter is approximately similar for ISAC–Barker and ISAC–Zadoff–Chu waveforms, as well as for ISAC–LFM waveform. However, as depicted in Figure 12, the clutter effect led to a deterioration in the velocity estimation performance of ISAC–Barker and ISAC–Zadoff–Chu waveforms at negative low speeds, while the performance of the ISAC–LFM waveform remained relatively consistent.

4.2 | Communication performance analysis for waveforms

In this section, the performance of the communication system is evaluated using different waveforms given in Figure 13. The communication receiver is designed according to the method given in Section 3.1. First the SER was analysed for all waveforms when $M = 4$. As can be seen in Figure 13, the performance of ISAC–Barker is quite low compared to other

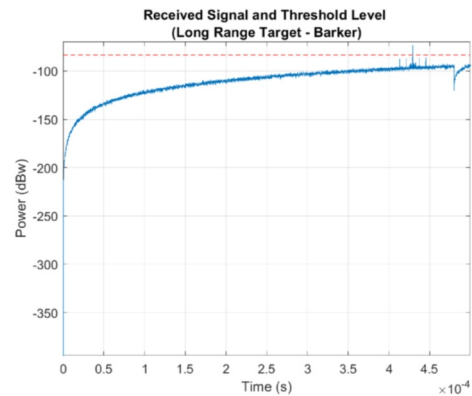


FIGURE 8 Received signal and threshold level for long range target—ISAC–Barker. ISAC, Integrated Sensing and Communications.

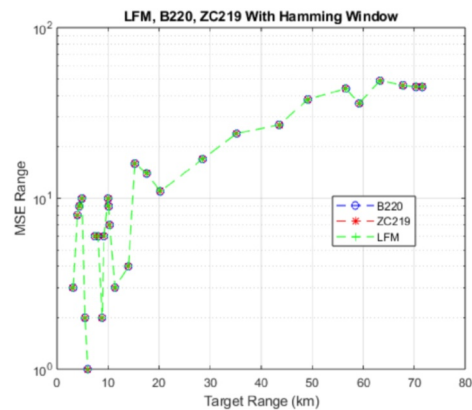


FIGURE 9 MSE range for ISAC–LFM, ISAC–Barker and ISAC–ZC with the Hamming window, $M = 4$, $BW = 11\text{MHz}$, $f_0 = 10\text{GHz}$. ISAC, Integrated Sensing and Communications; ISAC–LFM, Integrated Sensing and Communications–Linear Frequency Modulation; ISAC–ZC, Integrated Sensing and Communications–Zadoff–Chu; MSE, Mean square error.

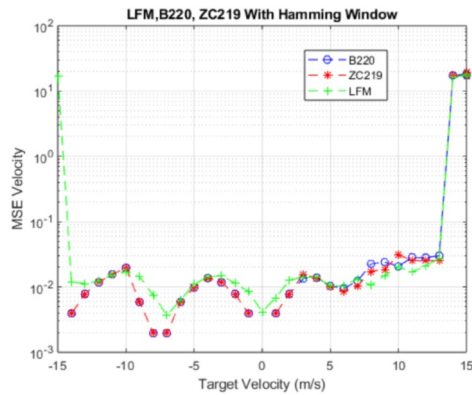


FIGURE 10 MSE velocity for ISAC-LFM, ISAC-Barker and ISAC-ZC with the Hamming window, $M = 4$, $BW = 11\text{MHz}$, $f_0 = 10\text{GHz}$. ISAC, Integrated Sensing and Communications; ISAC-LFM, Integrated Sensing and Communications-Linear Frequency Modulation; ISAC-ZC, Integrated Sensing and Communications-Zadoff-Chu; MSE, Mean square error.

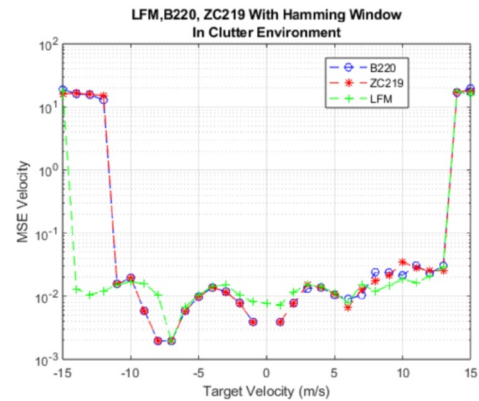


FIGURE 12 MSE velocity for ISAC-LFM, ISAC-Barker and ISAC-ZC with the Hamming window in the clutter environment, $M = 4$, $BW = 11\text{MHz}$, $f_0 = 10\text{GHz}$, $\text{rainrate} = 2\text{mm/hr}$. ISAC, Integrated Sensing and Communications; ISAC-LFM, Integrated Sensing and Communications-Linear Frequency Modulation; ISAC-ZC, Integrated Sensing and Communications-Zadoff-Chu; MSE, Mean square error.

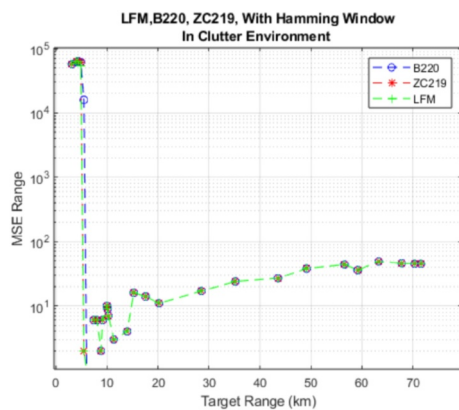


FIGURE 11 MSE range for ISAC-LFM, ISAC-Barker and ISAC-ZC with the Hamming window in the clutter environment, $M = 4$, $BW = 11\text{MHz}$, $f_0 = 10\text{GHz}$, $\text{rainrate} = 2\text{mm/hr}$. ISAC, Integrated Sensing and Communications; ISAC-LFM, Integrated Sensing and Communications-Linear Frequency Modulation; ISAC-ZC, Integrated Sensing and Communications-Zadoff-Chu; MSE, Mean square error.

waveforms. Although the performance of ISAC-ZC and ISAC-LFM waveforms is close for $M = 4$, ISAC-ZC shows slightly better performance than ISAC-LFM. In order to examine the performance of ISAC-ZC and ISAC-LFM waveforms in more detail, the analyses were repeated for $M = 16$. As can be seen in Figure 14, for $M = 16$, the performance of ISAC-ZC is quite good compared to ISAC-LFM.

5 | DISCUSSIONS

This study demonstrates the utilisation of phase modulation in ISAC systems, enabling the simultaneous use of a single waveform for both radar and communication functions throughout the transmission process. This approach allows both functions to effectively utilise the entire bandwidth of the joint waveform. The primary challenge lies in defining a

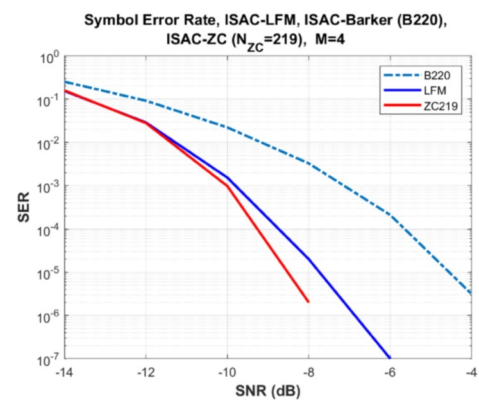


FIGURE 13 SER for ISAC-LFM, ISAC-Barker, ISAC-ZC for $M = 4$. ISAC, Integrated Sensing and Communications; ISAC-LFM, Integrated Sensing and Communications-Linear Frequency Modulation; ISAC-ZC, Integrated Sensing and Communications-Zadoff-Chu; SER, Symbol error rate.

waveform that offers high performance for both radar and communication purposes. In this context, the ISAC waveform has been defined using the Barker code, which is currently used in radar systems for both protection against intelligence and increasing radar range resolution. Additionally, the Zadoff-Chu sequence, known for its excellent periodic correlation properties and commonly used as a preamble in LTE communication systems, was selected for defining the ISAC waveform. It was hypothesised that this choice would not only ensure good performance in communication systems but also in radar systems, leveraging the shared properties of the Zadoff-Chu sequence.

The simulation results demonstrate that, thanks to the Hamming window employed in the radar receiver, phase-modulated ISAC waveforms exhibit comparable target detection performance to the frequency-modulated ISAC waveform. Furthermore, in the communication system, ISAC-Zadoff-Chu demonstrates superior SER performance

compared to both ISAC–Barker and ISAC–LFM. Since symbol detection in the communication receiver relies on cross-correlation, as outlined in Section 3.1, it is inferred that the superior performance of ISAC–Zadoff–Chu is attributed to its cross-correlation and autocorrelation characteristics [18, 19]. As can be seen in Figures 15–17, it is notable that the difference between the autocorrelation peak and the cross-correlation peak is most prominent for the ISAC-ZC waveform. Consequently, the ISAC-ZC waveform exhibits a superior SER compared to other waveforms.

The ISAC–Zadoff–Chu waveform exhibits admirable performance for both radar and communication functions. However, its implementation entails a more complex transmitter/receiver structure compared to ISAC–LFM. An FPGA-based Zadoff-Chu sequence generator is proposed in de Figueiredo et al. [20] (Figure 18). The coordinate rotation digital computer unit given in Figure 18 implements an iterative algorithm and includes multiple phase shifters and three adder units. The angle unit shown in Figure 18 consists of two sub-units, each containing multiple comparators. The translator unit converts α values into θ values by multiplying them by $2\pi/N_{ZC}$. Considering these operations performed in

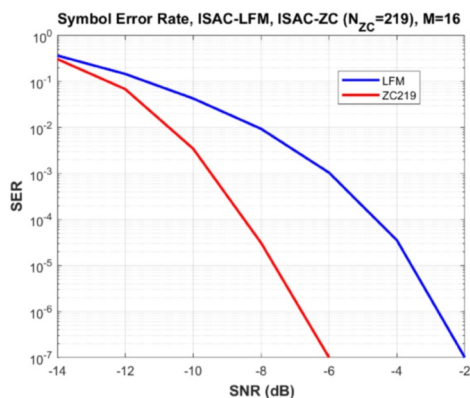


FIGURE 14 SER for ISAC-LFM, ISAC-ZC for $M = 16$. ISAC-LFM, Integrated Sensing and Communications-Linear Frequency Modulation; ISAC-ZC, Integrated Sensing and Communications-Zadoff-Chu; SER, Symbol error rate.

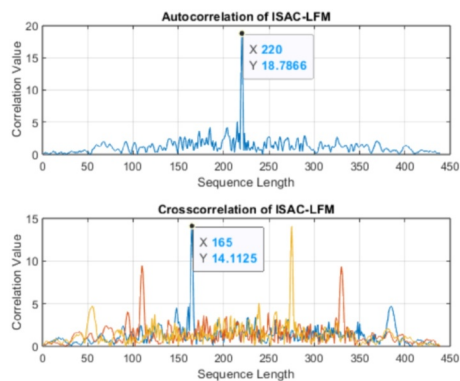


FIGURE 15 Autocorrelation and cross-correlation characteristic of ISAC-LFM for $SNR = 18dB$. ISAC-LFM, Integrated Sensing and Communications-Linear Frequency Modulation.

the ZC sequence generator, it can be noted that the structure of the generator proposed in de Figueiredo et al. [20] is more complex than an LFM generator (Figure 19) proposed in Kyeong-Rok Kim [21].

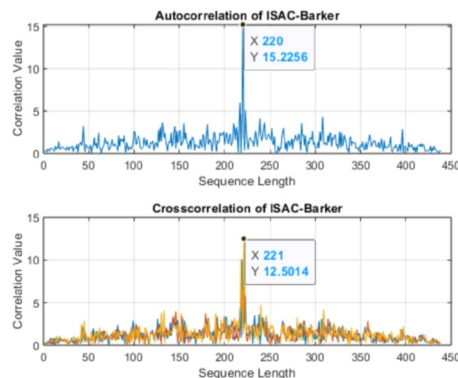


FIGURE 16 Autocorrelation and cross-correlation characteristic of ISAC-Barker for $SNR = 18dB$. ISAC, Integrated Sensing and Communications.

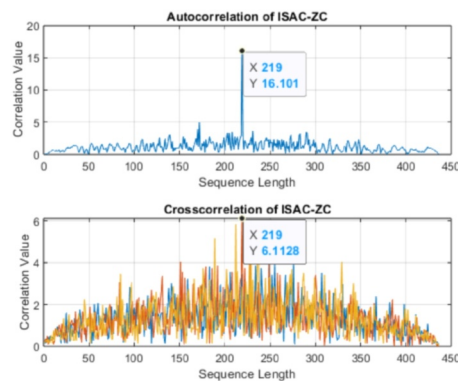


FIGURE 17 Autocorrelation and cross-correlation characteristic of ISAC-ZC for $SNR = 18dB$. ISAC-ZC, Integrated Sensing and Communications-Zadoff-Chu.

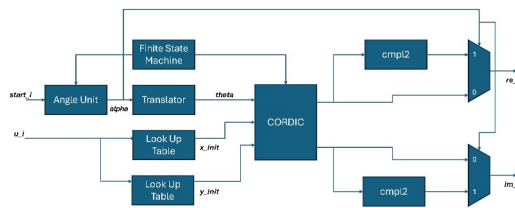


FIGURE 18 Architecture of the frequency domain Zadoff–Chu generator.

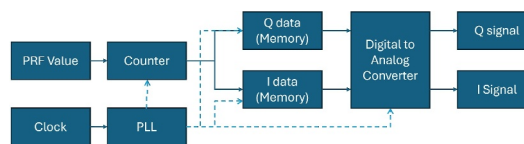


FIGURE 19 Memory-map-based Linear Frequency Modulated (LFM) waveform generator.

6 | CONCLUSIONS

In this study, we analysed the joint waveform of phase-coded pulses for both radar and communication performance in a mono-static pulse radar scenario for the ISAC system. We proposed an ISAC system that can execute both radar and communication functions with the same waveform using Barker and Zadoff–Chu sequences as the phase codes. Simulations were conducted by comparing the performance of ISAC–Barker and ISAC–Zadoff–Chu waveform with ISAC–LFM performance. As a result, it was observed that when phase-coded pulses are used as the ISAC joint waveform, the performance of the radar receiver is close in all three waveforms. On the other hand, when the performances in the communication receiver are compared, it is observed that the performance of ISAC-ZC stands out among the all waveforms. The ISAC-ZC waveform proposed within the scope of this study is considered highly promising for both radar and communication functions. In addition, in the Zadoff–Chu sequence, the ability to send a number of different communication symbols equal to one minus the code length without the need to change the instantaneous bandwidth of the signal also provides flexibility in the design of the communication system. Although the use of ISAC-ZC waveform causes a more complex structure in both the transmitter and receiver units, it is considered that it can be used in ISAC systems because its radar and communication performance is better than other waveforms. It is assessed that the ISAC-ZC waveform proposed in this study can be particularly useful in ISAC systems with high symbol data rate requirements, thereby enhancing the performance of both radar and communication functions. In future studies, it is aimed to study an optimisation algorithm in which the number of communication symbols is dynamically changed to optimise the performance of communication and radar systems in a variable scenario where the target range and the distance of the communication receiver change.

AUTHOR CONTRIBUTIONS

Sevda Şahin: Conceptualisation; Formal analysis; Software; Validation; Visualisation; Writing - original draft; Writing - review & editing. **Tolga Girici:** Conceptualisation; Formal analysis; Supervision; Visualisation; Writing - review & editing.

ACKNOWLEDGEMENTS

There are no funders to report for this submission.

CONFLICT OF INTEREST STATEMENT

The authors do not have a conflict of interest to disclose.

DATA AVAILABILITY STATEMENT

The data that support the findings of this study are available from the corresponding author upon reasonable request.

ORCID

Tolga Girici  <https://orcid.org/0000-0002-5705-4806>

REFERENCES

- Zheng, L., et al.: Radar and communication coexistence: an overview: a review of recent methods. *IEEE Signal Process. Mag.* 36(5), 85–99 (2019). <https://doi.org/10.1109/msp.2019.2907329>
- Noor-A-Rahim, M., et al.: Hybrid chirp signal design for improved long-range (LoRa) communications. *Signals* 3(1), 1–10 (2022). <https://doi.org/10.3390/signals3010001>
- Rodriguez-Garcia, P., et al.: Real-time synthesis approach for simultaneous radar and spatially secure communications from a common phased array. In: 2019 IEEE Radio and Wireless Symposium (RWS), pp. 1–4 (2019)
- Gehre, L., et al.: CP-DSSS for radar-centric integrated sensing and communication. In: 2023 20th European Radar Conference (EuRAD), pp. 347–350 (2023)
- Alabd, M.B., et al.: Time-frequency shift modulation for chirp sequence based radar communications. In: 2020 IEEE MTT-S International Conference on Microwaves for Intelligent Mobility (ICMIM), pp. 1–4 (2020)
- Şahin, S., Girici, T.: A novel radar receiver for joint radar and communication systems. In: 2023 International Conference on Radar, Antenna, Microwave, Electronics, and Telecommunications (ICRAMET), pp. 61–66 (2023)
- Rafique, S., Arslan, H.: A novel frame design for integrated communication and sensing based on position modulation. In: 2021 IEEE 94th Vehicular Technology Conference (VTC2021-Fall), pp. 1–5 (2021)
- Chunhong, Y., Zengli, L.: The superiority analysis of linear frequency modulation and barker code composite radar signal. In: 2013 Ninth International Conference on Computational Intelligence and Security, pp. 182–184 (2013)
- Wang, S., He, P.: Research on low intercepting radar waveform based on LFM and barker code composite modulation. In: 2018 International Conference on Sensor Networks and Signal Processing (SNSP), pp. 297–301 (2018)
- Sakshi Jain, J.V.O.: Contribution of barker and nested barker code in CDMA technology. *Int. J. Manag. Technol. Eng.* 8, 1633 (2018)
- Mahafza, B.R.: *Radar Signal Analysis and Processing Using Matlab*. Taylor & Francis Group (2009)
- Skolnik, M.I.: *Introduction to Radar Systems* 3/E. McGraw-Hill
- Andrews, J.G.: A primer on Zadoff Chu sequences. arXiv:221105702 [cs.IT] (2023)
- Diouri, O., et al.: Comparison study of hardware architectures performance between FPGA and DSP processors for implementing digital signal processing algorithms: application of FIR digital filter. *Results Eng.* 16, 100639 (2022). <https://doi.org/10.1016/j.rineng.2022.100639>
- Sloss, A.N., Symes, D., Wright, C.: *ARM System Developers Guide*. Morgan Kaufmann Publishers (2004)
- Antonijević, G., et al.: An approach of generating and matched filtering of modulated radar signals using the FPGA. *Scientific Technical Rev.* 68(3), 43–49 (2018). <https://doi.org/10.5937/str1803043a>
- Mirghani, M.: Implementation of Matched Filters Using Microcontrollers, pp. 128–132 (2016)
- Vanita, B., Kaba, R.R.P.: A precoding based PAPR minimization schemes for NOMA in 5G network. *SN Comput. Sci.* 2(4), 262 (2021). <https://doi.org/10.1007/s42979-021-00639-z>
- Park, D.S., et al.: A satellite navigation signal scheme using zadoff-chu sequence for reducing the signal acquisition space. *J. Position. Navig. Timing* 2(1), 1–8 (2013). <https://doi.org/10.11003/jkgs.2013.2.1.001>
- de Figueiredo, F.A., et al.: Efficient FPGA-based implementation of a CAZAC sequence generator for 3GPP LTE. In: 2014 International Conference on ReConfigurable Computing and FPGAs (ReConFig14), pp. 1–6. IEEE (2014)
- Kyeong-Rok Kim, J.H.K.: Wideband waveform generation using MDDS and phase compensation for X-band SAR. *Rem. Sens.* 12(9), 1431 (2020). <https://doi.org/10.3390/rs12091431>

How to cite this article: Şahin, S., Girici, T.: Phase coded waveforms for integrated sensing and communication systems. *IET Radar Sonar Navig.* 18(12), 2608–2616 (2024). <https://doi.org/10.1049/rsn2.12661>